RSC Advances

PAPER

View Article Online
View Journal | View Issue

Cite this: *RSC Adv.*, 2021, **11**, 31756

Polytorsional-amide/carboxylates-directed Cd(II) coordination polymers exhibiting multi-functional sensing behaviors†

Jie Chi,‡[a] Yajun Mu,‡[a] Yan Li,[a] Pengpeng Shao,[b] Guocheng Liu, *[ab] Bin Cai, *[c] Na Xu[a] and Yongqiang Chen *[d]

Received 7th June 2021
Accepted 19th September 2021

DOI: 10.1039/d1ra04411g

rsc.li/rsc-advances

By rational assembly of polytorsional-amide [*N*,*N*′-bis(4-methylenepyridin-4-yl)-1,4-naphthalene dicarboxamide (**L**)] and polytorsional-carboxylates [H_2ADI = adipic acid, H_2PIM = pimelic acid, H_2SUB = suberic acid], three new Cd-based coordination polymers (CPs) $C_{30}H_{30}CdN_4O_7$ (**1**), $C_{31}H_{32}CdN_4O_7$ (**2**) and $C_{31.03}H_{30.55}CdCl_{0.24}N_4O_{5.52}$ (**3**) were successfully synthesized. CPs **1–2** and **3** are 2D networks and a 3D framework, which all display 3,5-connected topologies with different structural details. The effects of carboxylates with different carbon chains on the structure of the complexes were studied. Fluorescence experiments show that CPs **1–3** have good multi-functional sensing ability for metal cations (Fe^{3+}), anions (MnO_4^-, CrO_4^{2-}, $Cr_2O_7^{2-}$) and organochlorine pesticides (2,6-dichloro-4-nitroamine) with good anti-interference and recyclable characteristics. The possible sensing mechanism is also investigated in detail.

1. Introduction

With the rapid development of industrialization and agriculture in the world, more and more wastewater is discharged without rational treatment, causing heavy metal and organic pollution in the ecological environment.[1–4] Common heavy metal elements include Fe, Cr, Mn, *etc.*[5,6] Iron is an essential trace element for the human body, but excessive intake will endanger health, and because of its long-lasting toxicity, it will lead to metabolic disorder and increase the risk of cardiovascular disease and cancer.[7–10] Chromium usually exists in the form of CrO_4^{2-} and $Cr_2O_7^{2-}$. Hexavalent chromium is an inhalant poison, which is one of the most allergenic metal elements.[11–13] It is easily absorbed by human body and has carcinogenic effect in specific parts such as lung and nasal cavity.[14,15] Potassium permanganate is a strong oxidizing substance, which is often used in daily life to disinfect and remove peculiar smell.[16] However, when the concentration is too high, it is irritating and corrosive, which will burn the skin, and 10 g is the lethal dose.[17–20] In addition, in order to improve the quality and yield of crops in the agricultural production process, a proper amount of pesticides will be added, but with the continuous increase of the dosage, serious pesticide pollution will be caused.[21–24] The use of pesticides not only benefits human beings, but also harms the environment on which human beings live. Therefore, it is of great significance to the reasonable detection of the above pollutants.

In recent years, many instrumental methods for rapid detection of these pollutants have been developed, but their practical application is limited due to the disadvantages of high cost, complicated equipment and large relative error.[25–28] Therefore, it is necessary to develop new efficient and simple detection method to realize simultaneous detection of multiple components. Fluorescence sensing is an effective method to detect various pollutants at present.[29,30] Among many fluorescent sensing materials, coordination polymers (CPs) self-assembled by d^{10} metal centers and organic ligands are considered as a kind of excellent sensor used for qualitative and quantitative detection of heavy metal ions, organic pesticides, antibiotic.[31–37] However, some of these sensors have relatively single detection objects.[38–40] Thus, it is of great significance to develop complex-based sensing materials with multifunctional detection response, which is also a challenge facing this field at present.[41,42] Owing to the selectivity of coordination between metal and ligand, it is difficult for some rigid organic ligands to meet the coordination needs of metal ions.[43–45] Fortunately,

[a]*College of Chemistry and Materials Engineering, Professional Technology Innovation Center of Liaoning Province for Conversion Materials of Solar Cell, Bohai University, Jinzhou 121013, P. R. China. E-mail: lgch1004@sina.com*

[b]*Key Laboratory of Cluster Science Ministry of Education, Beijing Key Laboratory of Photoelectronic/Electrophotonic, Advanced Research Institute of Multidisciplinary Science, School of Chemistry and Chemical Engineering, Beijing Institute of Technology, Beijing 100081, P. R. China*

[c]*School of Chemistry and Chemical Engineerng, Zhoukou Normal University, Zhoukou 466001, P. R. China. E-mail: caib@actinide.org*

[d]*College of Chemistry and Chemical Engineering, Jinzhong University, Jinzhong, Shanxi, 030619, P. R. China. E-mail: chenjzxy@126.com*

† Electronic supplementary information (ESI) available. CCDC 2071312–2071314. For ESI and crystallographic data in CIF or other electronic format see DOI: 10.1039/d1ra04411g

‡ Jie Chi and Yajun Mu contributed equally to this work.

proper selection of flexible ligands is an effective strategy to meet the coordination needs of metal ions.[46,47] As a kind of flexible ligands, propanedioic acid, succinic acid, glutaric acid, adipic acid, pimelic acid and suberic acid have polymethylene $-(CH_2)_n-$ that exhibit polytorsional characteristics and conformational flexibility. It may lead to unpredictable structural diversity, which is conducive to exploring the relationship between structure and properties.[48–50]

Based on the above considerations, three fatty dicarboxylic acids [H_2ADI = adipic acid, H_2PIM = pimelic acid, H_2SUB = suberic acid] and a bis-pyridine amide *N*,*N*′-bis(4-methylenepyridin-4-yl)-1,4-naphthalene dicarboxamide (**L**) were selected to combine with d^{10} metal ion (Cd^{2+}). The polytorsional features of the above fatty carboxylates and neutral ligands owing to the different amount of methylene groups is beneficial to meet the coordination needs of Cd^{2+}, and to improve the crystallinity of CPs.[51] The appropriate σ electron donating ability and π electron accepting ability of **L**, and the multi-potential recognition sites of **L** derived from its amides, will be beneficial to show the characteristics of its multifunctional response.[52,53] As a result, three new Cd-based coordination polymers $C_{30}H_{30}CdN_4O_7$ (**1**), $C_{31}H_{32}CdN_4O_7$ (**2**) and $C_{31.03}H_{30.55}CdCl_{0.24}N_4O_{5.52}$ (**3**) were successfully synthesized, which display 2D 3,5-connected networks of CP **1** and CP **2**, and 3D 3,5-connected framework of CP **3**. The effects of carboxylates with different spacer's length and the polytorsional features of the N-/O-donors on the structure of the title CPs were studied. Fluorescence experiments show that CPs **1–3** have good multifunctional sensing ability for metal cations (Fe^{3+}), anions (MnO_4^-, CrO_4^{2-}, $Cr_2O_7^{2-}$) and organochlorine pesticides (2,6-dichloro-4-nitroamine) with good LOD and K_{sv}. The sensing mechanism is also investigated in detail.

2. Experimental

2.1 Materials and methods

For more detailed information about methods and materials, please refer to ESI.†

2.2 Preparation of 1–3

$CdCl_2 \cdot 5/2H_2O$ (0.0457 g, 0.2 mmol), **L** (0.0394 g, 0.1 mmol), adipic acid (0.0292 g, 0.2 mmol) dissolve in distilled H_2O (6 mL) and NaOH (0.1 mol L^{-1}, 4 mL), the mixture was placed in a 25 mL Teflon-lined stainless steel autoclave and then reacted at 120 °C for 4 days. After cooling to room temperature, colorless crystals were obtained in 24% yield based on **L**. Anal. calcd (%) for $C_{30}H_{30}CdN_4O_7$: C 53.72, H 4.48, N 8.36. Found: C 53.70, H 4.51, N 8.35. IR (KBr, cm^{-1}): 3517 w, 3389 w, 3049 w, 2926 m, 1632 s, 1554 s, 1426 s, 1298 m, 1258 w, 1145 w, 1018 m, 968 w, 856 w, 790 m, 628 w (Fig. S1†). The synthetic process for **2** and **3** are the similar to that of **1** except that H_2ADI was superseded by H_2PIM and H_2SUB and 2 mL DMA solution was added to the mixed system (for detailed steps, please refer to ESI†). The crystallization and refinement data for CPs **1–3** are shown in Table 1. CCDC numbers: 2071313 (**1**), 2071314 (**2**), 2071312 (**3**).

2.3 X-ray crystallography

The crystal data of CPs **1–3** are shown in Tables 1 and S1–S3.† The details about X-ray crystallography are list in ESI.†[54]

2.4 The process of the fluorescent experiment for CPs 1–3

The process of the fluorescent experiment are referred to the reported method.[55–57] The CPs **1–3** were ball-milled and the SEM was used to show the morphology before they were prepared

Table 1 Crystal and refinement data for complexes **1–3**

Complexes	**1**	**2**	**3**
Empirical formula	$C_{30}H_{30}CdN_4O_7$	$C_{31}H_{32}CdN_4O_7$	$C_{31.03}H_{30.55}CdCl_{0.24}N_4O_{5.52}$
Fw	670.98	685.00	681.01
Crystal system	Triclinic	Triclinic	Triclinic
Space group	$P\bar{1}$	$P\bar{1}$	$P\bar{1}$
a (Å)	8.9887 (3)	10.4592 (6)	9.3563 (18)
b (Å)	10.5199 (4)	11.9988 (7)	9.873 (2)
c (Å)	17.3822 (6)	12.1578 (7)	17.234 (3)
α (°)	79.3500 (10)	95.7890 (10)	77.943 (4)
β (°)	76.9520 (10)	97.0530 (10)	75.068 (4)
γ (°)	67.5230 (10)	91.2190 (10)	71.533 (4)
V (Å^3)	1470.22 (9)	1505.63 (15)	1444.9 (5)
Z	2	2	2
D_{calc} (g cm^{-3})	1.516	1.511	1.537
μ (mm^{-1})	0.796	0.779	0.827
F(000)	684.0	700.0	682.0
R_{int}	0.0143	0.0214	0.0466
$R_1{}^a$ [$I > 2\sigma(I)$]	0.0300	0.0387	0.0619
$wR_2{}^b$ (all data)	0.0805	0.0842	0.1521
GOF	1.029	1.006	0.999
$\Delta\rho_{max}$ (e Å^{-3})	0.70	0.62	1.050
$\Delta\rho_{min}$ (e Å^{-3})	−0.65	−0.43	−0.775

^{a} $R_1 = \Sigma||F_o| - |F_c||/\Sigma|F_o|$. ^{b} $wR_2 = \Sigma[w(F_o^2 - F_c^2)^2]/\Sigma[w(F_o^2)^2]^{1/2}$

into suspension (Fig. S2†). In the fluorescence sensing experiment, 3 mg crystal powder was soaked in cationic, anionic solution and organochlorine pesticides. The experiments for selectivity and anti-interference, the fluorescence titration experiment for quantitative analysis are all based on the corresponding fluorescence intensity. The details are listed in ESI.†

3. Result and discussion

3.1 Description of structural features for CPs 1–3

The single crystal X-ray diffraction analysis shows that CPs **1–3** are all crystallized in triclinic system with $P\bar{1}$ space group. In **1** and **2**, each Cd^{2+} is six-coordinated by four carboxylic O atoms and two N atoms from the pyridyls of **L** (Chart 1a). The Cd–O distances are in the range of 2.281 (2) Å to 2.4618 (19) Å. Cd–N distances are from 2.329 (2) to 2.376 (2) Å (Tables S1 and S2†). Two Cd^{2+} are linked by two O atoms from ADI (for **1**) or PIM (for **2**) forming bimetallic subunits. The adjacent subunits are bridged by pairs of ADI (for **1**) or PIM (for **2**) to generate 1D Cd-carboxylate-bands (Chart 1b). The parallel bands are further connected into a 2D networks by pairs of **L** ligands (Chart 1c and d). Taking the bimetallic clusters as nodes, **1** and **2** display (3,5)-connected 2D networks extended by **L** and double linkers of carboxylates (Chart 1e). The Cd^{2+} in **3** is coordinated with two pyridyl N atoms and an amide O atom of three different **L**, two carboxylic O atoms, part of Cl^- (occupancy 0.242) and part of O atom from SUB (occupancy 0.758) (Chart 1a). The Cd–O distances are in the range of 2.262 (8) Å to 2.486 (7) Å. The Cd(1)–Cl(1) distance is 2.430 (11) Å. The Cd–N distances are from 2.340 (7) to 2.335 (7) Å (Table S3†). All the distances of the coordinated bonds Cd-involved in **1–3** are in the reasonable range.[58–61] Each Cd^{2+} coordinated with three **L** ligands and about two SUB anions, each **L** ligand bridged three Cd^{2+}. Thus, **3** exhibits a (3,5)-connected 3D framework associated with the point symbol of $\{4^2\cdot6^5\cdot8^3\}\cdot\{4^2\cdot6\}$ (Chart 1e).

3.2 The synergistic coordination effects of polytorsional amides/carboxylates on the structures of the title CPs

In-depth structural analysis shows that the spacers of carboxylates have obvious guiding effect on the structures of the title

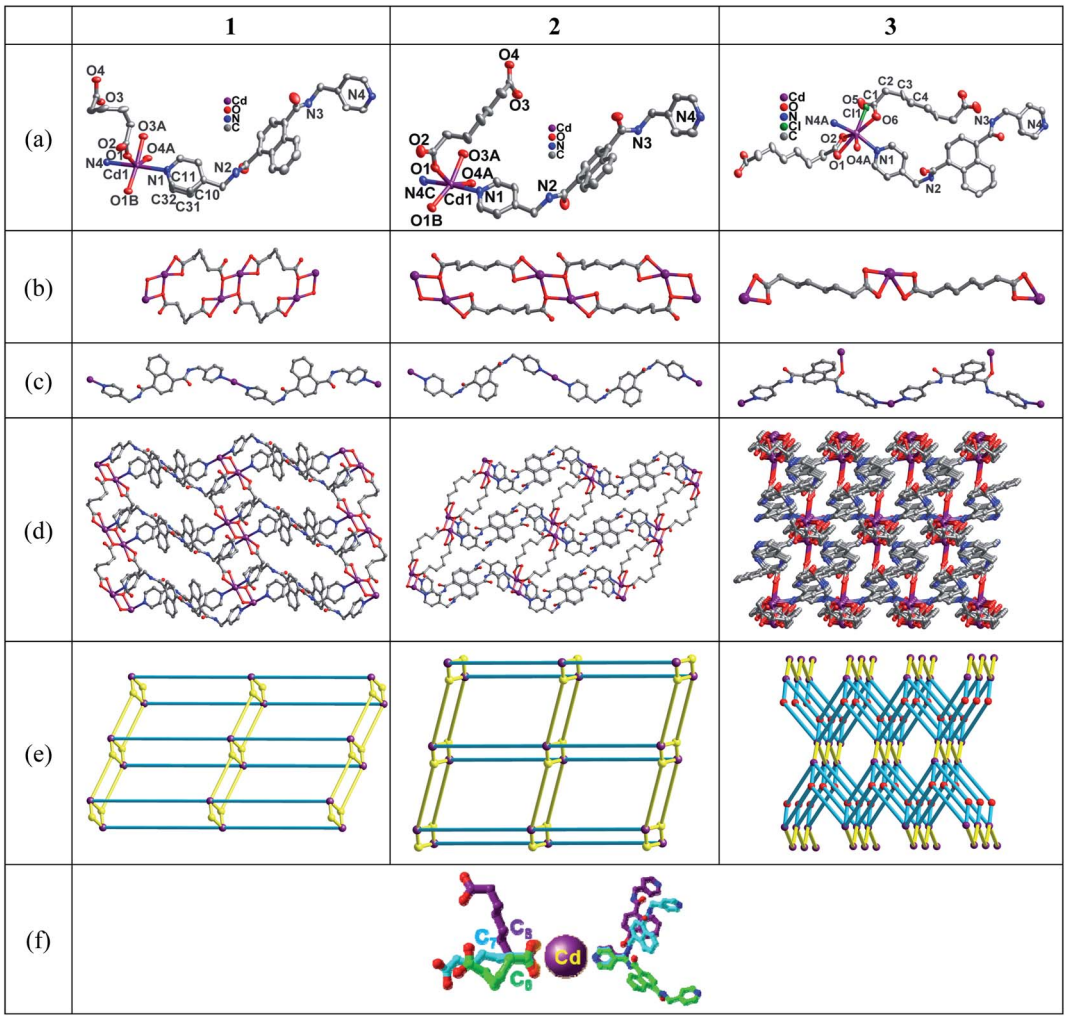

Chart 1 The crystalline structure of CPs **1–3**. (a) The coordination environment of Cd(II) ions in CPs **1–3** (ellipsoid percent: 50%, C10, C11, C31 and C32 in **1** and Cl1, O5, O6, C1, C2, C3 and C4 in **3** are disordered). (b) Metal–dicarboxylate units. (c) 1D $[Cd\text{-}L]_n$ chains. (d) Two-dimensional structure of CPs **1–2** and three-dimensional framework of CP **3**. (e) The topology structures. (f) Polytorsional features of amides and carboxylates in **1–3**.

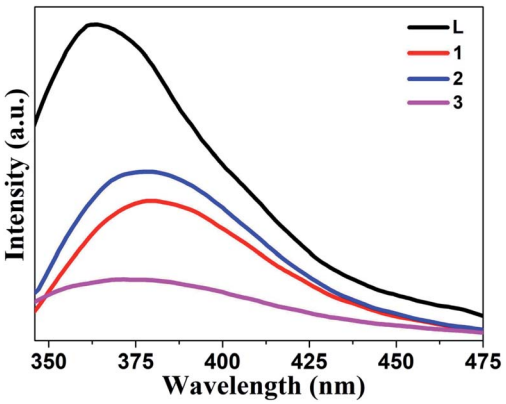

Fig. 1 Fluorescence spectra of CPs 1–3 and L in solid state.

complexes. In the title complexes, the numbers of $-CH_2-$ spacers of ADI, PIM and SUB are changed from 4 to 6, which lead to different coordination characteristics. The ADI, PIM and SUB display μ_2–η^0:η^2/μ_1–η^1:η^1, μ_2–η^0:η^2/μ_1–η^1:η^1 and μ_1–η^1:η^1/μ_1–η^1:η^1 coordinated modes. The Cd···Cd distances linked by the corresponding carboxylates are from 8.989 Å, 12.158 Å to 11.881 Å. These coordinated features induce to form the 1D double-chains of Cd-ADI/PIM-subunits in **1** and **2**, and a single chain of Cd-SUB subunit in **3**. In order to meet the different coordination requirements of the above structural subunits, the metal ions and amide ligands show excellent synergistic coordination adaptability. The coordination numbers of Cd^{2+} are tuned from 6 in **1** and **2** to 7 in **3**. The dihedral angles of two pyridine rings of **L** are 37.34°, 47.48° and 33.46°. The Cd···Cd distances connected by the **L** are from 20.44 Å, 20.11 Å to 17.98 Å. The above structural features lead to the (3,5)-connected 2D networks of **1** and **2**, and (3,5)-connected 3D framework of **3**.

3.3 Photoluminescence properties

All complexes are composed of pyridine amide ligand **L** and d^{10} metal ions, which have excellent fluorescence properties.[62] In order to further explore the luminescence sensing of these CPs, the solid-state luminescence spectra of the title complexes and free ligand **L** were systematically studied. As shown in Fig. 1, at 364 nm, it shows the maximum emission peak of **L**, which is caused by $\pi^* \rightarrow \pi$ transitions.[63] Similarly, three new Cd-based CPs also showed similar luminescence, and a slight red shift was observed. The emission spectra of CPs **1–3** are shown at

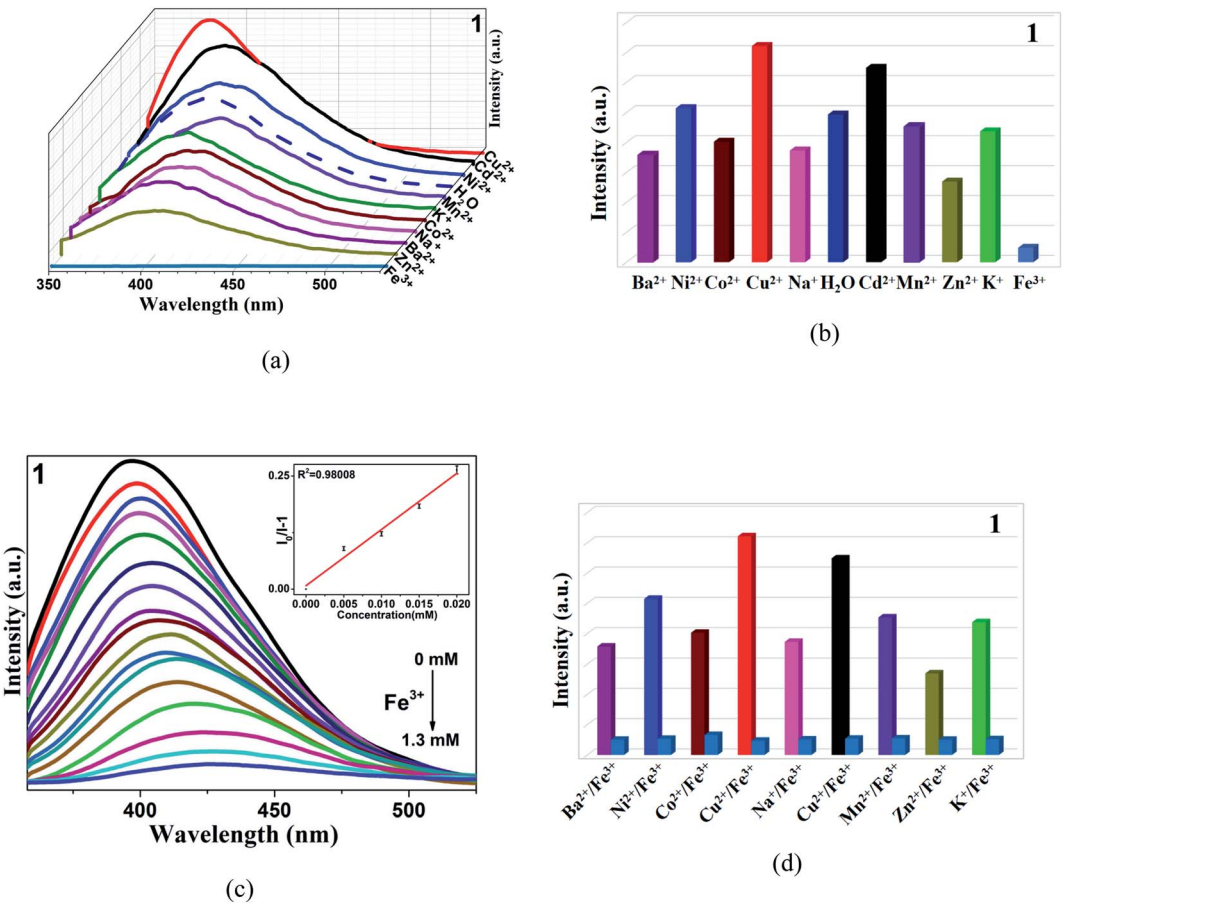

Fig. 2 (a) Fluorescence intensity spectra of CP **1** dispersed in different metal cations (waterfall plot). (b) Emission intensity of CP **1** in various metal cations (histogram). (c) Adding Fe^{3+} solutions with different volume (concentrations of 10^{-3} M), the fluorescence intensity of CP **1** (inset: at low concentrations, linear relationship between $I_0/I - 1$ and analyte concentration). (d) The selectivity of CP **1** to Fe^{3+} solution is interfered by other metal cations.

Table 2 Sensing properties of 1–3

	Analytes	1	2	3
K_{sv} (M^{-1})	Fe^{3+}	1.202×10^4	1.189×10^4	1.734×10^4
	MnO_4^-	1.794×10^4	2.158×10^4	2.506×10^4
	CrO_4^{2-}	1.987×10^4	2.399×10^4	2.323×10^4
	$Cr_2O_7^{2-}$	3.055×10^4	2.922×10^4	1.629×10^4
	2,6-DC-4-NA	1.334×10^5	1.609×10^5	2.483×10^5
LOD (μM)	Fe^{3+}	630	710	730
	MnO_4^-	420	390	510
	CrO_4^{2-}	380	350	550
	$Cr_2O_7^{2-}$	250	290	780
	2,6-DC-4-NA	57	52	51

379 nm, 379 nm and 372 nm, respectively. The fluorescence emission of **1–3** may be due to $\pi^* \rightarrow \pi$ and $n \rightarrow \pi^*$ transitions in ligands.[18] In addition, the fluorescence intensity of CPs **1–3** relative to free ligand is obviously weakened and they are different from each other, which may be caused by the difference of structures and carboxylic units.

3.4 Selective sensing of metal cations

As we all know, the composition and structure of the complexes will have some effect on the final properties.[64] CPs **1–3** use the same metal ions and organic ligands and combine with different carboxylic acids. Therefore, the fluorescence sensing characteristics of three complexes to different metal cations in aqueous solution were studied to explore their differences in properties. First of all, in order to fully integrate the complexes with the aqueous solution, they were finely ground. Weighed 3 mg powder and dispersed them into 3 mL $M(Cl)_x$ ($M = Ba^{2+}$, Ni^{2+}, Co^{2+}, Cu^{2+}, Na^+, Cd^{2+}, Mn^{2+}, Fe^{3+}, Zn^{2+}, K^+) aqueous solution with the same concentration (10^{-2} M), and then ultrasonic treatment for about 40 minutes. From Fig. 2, CP **1** reveals selective quenching response to Fe^{3+}, but there is no obvious reaction to other cations. And the same phenomenon was observed in other complexes (Fig. S4 and S5†). After that, the sensitivity of complexes to Fe^{3+} were evaluated by quantitative titration experiment, in Fig. 2c, Fe^{3+} solutions with different volumes and concentrations of 10^{-3} M were added to the aqueous suspension. The results showed a good linear relationship in the low concentration range. The quenching constants were calculated by Stern–Volmer (S–V) equation $K_{sv} = [I_0/I - 1]/C$ (I_0 = the initial fluorescence intensity, I = the final fluorescence intensity after quenching, C = the molar concentration of the analyte).[65] The K_{sv} values of CPs **1–3** are 1.202×10^4 M^{-1}, 1.189×10^4 M^{-1} and 1.734×10^4 M^{-1}, the detection limits are shown in the Table 2. Shi, Hu and Hou's groups have been investigated various complex-based sensors for Fe^{3+}.[66–68] Compared with some reported coordination polymers, the quenching constant of the target compounds are comparable or even better (Table S4†).

In order to explore the selectivity of detecting Fe^{3+} ions compared with other interfering metal ions, competitive experiments were conducted. Adding other metal ions into CP **1**, and then adding Fe^{3+} into the mixed solution, the fluorescence intensity quenching was remarkable (Fig. 2d), which indicates that CP **1** can effectively and selectively sense Fe^{3+} without interference from other metal ions. Similar phenomena were found in CPs **2** and **3** (Fig. S4d and S5d†).

3.5 Selective sensing of anions

To study whether CP **1** can be used as a fluorescence probe for detecting anions, the samples were dispersed in different aqueous solutions of anions (OH^-, HCO_3^-, NO_3^-, Br^-, CO_3^{2-}, I^-, CH_3COO^-, MnO_4^-, CrO_4^{2-}, $Cr_2O_7^{2-}$) and K^+ according to the same method as above, and the changes of fluorescence intensity were observed. It is worth noting that these selected anions have different effects on the fluorescence intensity of the complexes. Three anions (MnO_4^-, CrO_4^{2-}, $Cr_2O_7^{2-}$) have higher quenching efficiency for complexes by comparison (Fig. 3). Then, a gradient experiment was carried out (Fig. 4). Taking CP **1** as an example, with the aqueous solutions of three anions gradually added to the blank suspension of the complex, the luminescence intensity of **1** changed rapidly. According to the formula $[I_0 - I]/I_0 \times 100\%$ (I and I_0 are the same as mentioned above), the quenching efficiency is 94.1% for MnO_4^-, 97.9% for CrO_4^{2-} and 97.4% for $Cr_2O_7^{2-}$, respectively. The S–V diagram obtained in the low concentration range, the K_{sv} values were calculated (Table 2). In addition, the detection limits (LOD = $3\sigma/K_{sv}$) of CP **1** for MnO_4^-, CrO_4^{2-} and $Cr_2O_7^{2-}$ were calculated based on the K_{sv} value and standard deviation (σ) of repeated

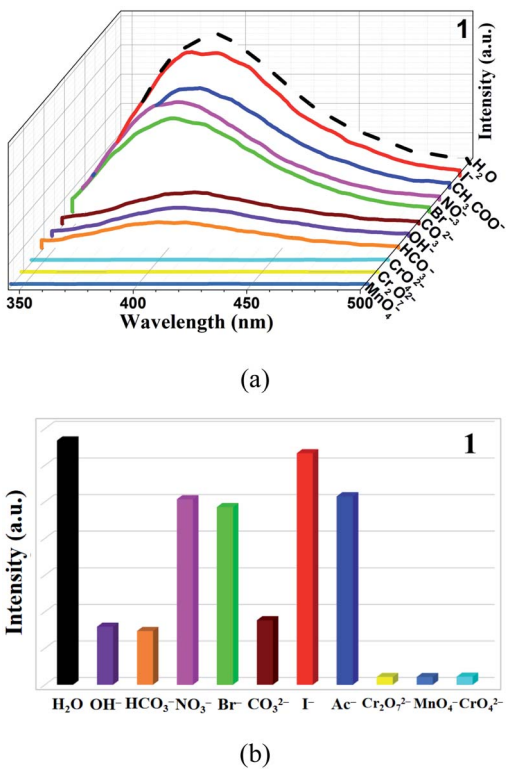

Fig. 3 (a) Fluorescence intensity spectra of CP **1** dispersed in different anions (waterfall plot). (b) Emission intensity of CP **1** in various anions (histogram).

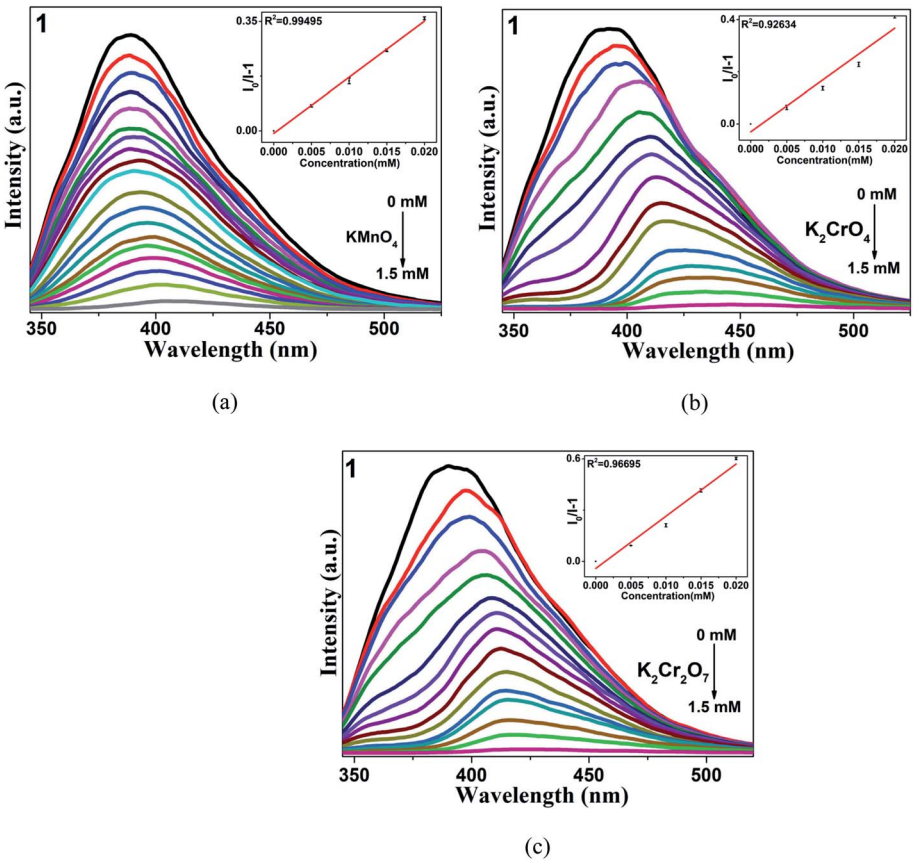

Fig. 4 The fluorescence intensity of CP **1**, adding MnO_4^- (a), CrO_4^{2-} (b) and $Cr_2O_7^{2-}$ (c) solutions with different volumes and concentrations of 10^{-3} M (inset: at low concentrations, linear relationship between $I_0/I - 1$ and analyte concentration).

fluorescence measurement of blank solution, and listed in the Table 2.[11] Yong and Cui's groups synthesized several complexes for the detection of anions.[69,70] In contrast, the target complexes have higher fluorescence quenching constants, which are of great significance for the detection of anions (Table S5†). Considering the practical application, there are many kinds of anions in the wastewater treatment process, so anti-interference experiments should be carried out.[29] Satisfactory, in the presence of other anions, the fluorescence intensity decreased to a great extent, which indicated that the quenching ability of CP **1** was not interfered by other anions (Fig. 5).

3.6 Selective sensing of organochlorine pesticides

Some pesticides used at present can be biodegraded into harmless substances in a short time, while some organochlorine pesticides are difficult to degrade.[71,72] And excessive pesticide residues will directly endanger the nervous system of the human body and important organs such as liver and kidney. Therefore, it is important to find a suitable and easy-to-operate method to detect such substances. Because the selected four pesticides are insoluble in water, they are dissolved in ethanol.[23] Firstly, the fluorescence intensity of CP **1** in ethanol solution was determined, and it was found that the fluorescence intensity was similar to that in water. The results showed that ethanol solvent has little effect on its fluorescence intensity. 3 mg crystal powder was added into the mixed solution of complexes and ethanol, then added atrazine (AT), 1,2,3-trichlorobenzene (1,2,3-TCB), 1,2,4,5-tetrachlorobenzene (1,2,4,5-TCB), 2,6-dichloro-4-nitroamine (2,6-DC-4-NA) respectively. As shown in Fig. 6, compared with other pesticides, 2,6-DC-4-NA showed the greatest fluorescence quenching intensity. Therefore, in order to study the sensing characteristics of 2,6-DC-4-NA in detail, pesticide solution with a concentration of 10^{-3} M was continuously added to the blank solution. With the increase of solution volumes, the fluorescence intensity of **1** gradually decreased, and when 500 μL was added, the intensity was almost completely quenched. The quenching constant of CP **1**

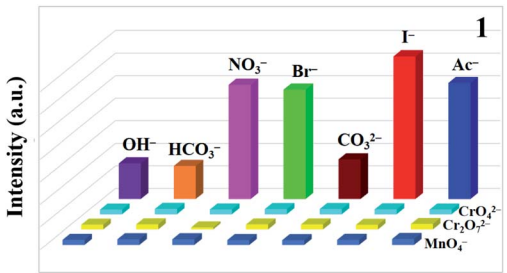

Fig. 5 The anti-interference experiment of CP **1**, in the presence of MnO_4^-, CrO_4^{2-} and $Cr_2O_7^{2-}$ solutions.

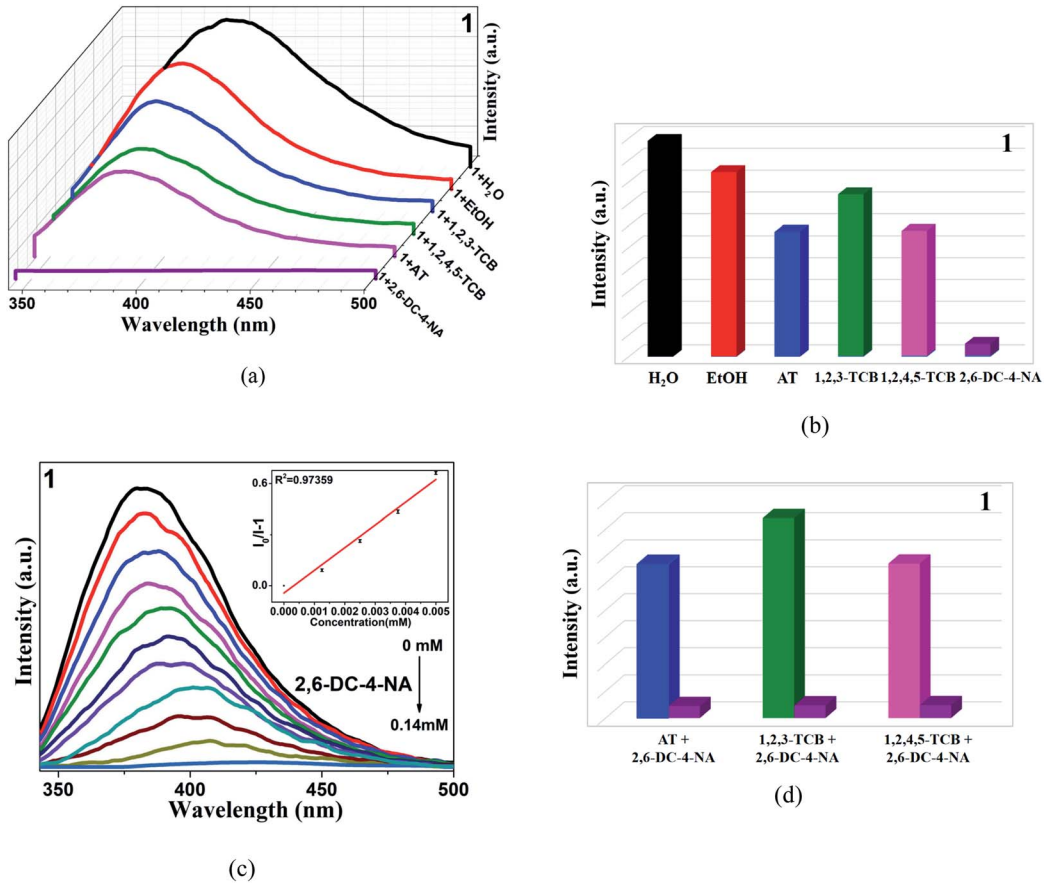

Fig. 6 (a) Fluorescence intensity spectra of CP **1** dispersed in several pesticides (waterfall plot). (b) Emission intensity of CP **1** in different pesticides (histogram). (c) Fluorescence spectra of CP **1** to pesticides with different volumes in ethanol solution (inset: at low concentrations, linear relationship between $I_0/I - 1$ and analyte concentration). (d) The anti-interference experiment.

was calculated by quenching S–V equation (Table 2). Liu and Halder have been investigated the detection for 2,6-DC-4-NA by coordination polymers.[23,55,73] As shown in Table S6,† the higher quenching constant and lower detection limit further confirm that CPs **1–3** are good candidates for pesticide detection sensors. Similarly, anti-interference experiments were also carried out, the above results confirm that these three complexes have a little high selectivity and anti-interference ability to 2,6-DC-4-NA.

As we all know, the stability and recoverability of fluorescence sensor are very important indexes in actual detection. Taking **1** as an example, the crystal powder was soaked in Fe^{3+}, MnO_4^-, CrO_4^{2-}, $Cr_2O_7^{2-}$ and 2,6-DC-4-NA solutions for 24 hours, and the obtained spectra were compared with the original spectra by powder X-ray diffraction and single-crystal X-ray diffraction. It was found that they were basically consistent, which proved that the structure of the complex has not changed significantly after fluorescence detection (Fig. S3†). In addition, the cyclic properties of the complexes for these detected substances were also studied. As shown in Fig. S13,† after three cycles, the change of fluorescence quenching efficiency of the complexes were almost negligible. At the same time, in order to verify the reproducibility of the fluorescence sensing experiment, three parallel experiments of quantitative titration were carried out, and the average value and relative standard deviation of the repeated experiments were calculated. The range of RSD obtained was 0.48–1.67% in this manuscript. All the data are within a reasonable range.[74,75] The results showed that the experimental process has relatively high precision and good repeatability (Tables S7–S9†). Although the title complexes have good selectivity and detection limit as fluorescence sensors, there is still a long way to go to apply them to commercial detection reagents. How to realize the commercialization of materials by optimizing the shape, size and testing environment of materials and reducing the cost of materials will be the direction of our future efforts, and there will be great challenges.

3.7 Mechanism of fluorescence sensing

The possible mechanism of luminescence quenching of different analytes was further studied. According to previous studies, it is found that most possible quenching mechanisms are skeleton collapse, charge transfer and energy transfer.[66,76] Taking CP **1** as an example, firstly, the PXRD of **1** was determined after soaking in different analytes for 24 hours. The Fig. S3a† showed that there was almost no difference in PXRD of

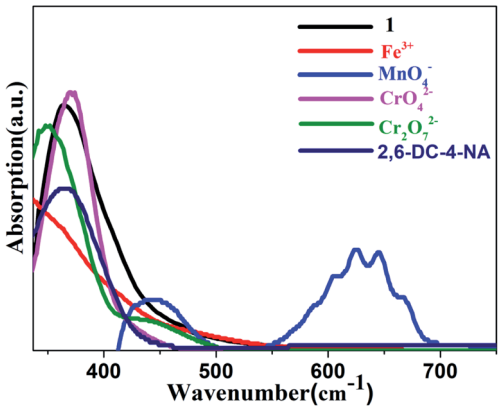

Fig. 7 The UV-vis absorption spectra of five analytes and emission spectra of **1**.

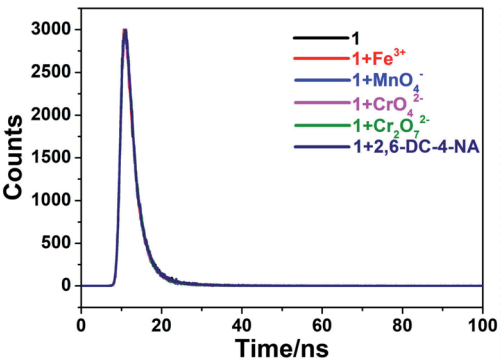

Fig. 8 Lifetime decay curves of **1** before and after the addition of five analyses.

1 before and after fluorescence detection, indicating that fluorescence quenching was not caused by the collapse of the framework. Then, the UV-vis absorption spectra of five analytes were tested. As shown in Fig. 7, the absorption spectra of these analytes partially overlap with the emission spectra of CP **1**, indicating that energy can be effectively transferred from the complex to the analytes, resulting in resonance energy transfer.[77] In addition, the fluorescence lifetime of **1** before and after adding analytes were measured, and the fluorescence lifetime were calculated to be 3.11 ns (**1**), 3.07 ns (**1** + Fe^{3+}), 2.99 ns (**1** + MnO_4^-), 2.94 ns (**1** + CrO_4^{2-}), 2.97 ns (**1** + $Cr_2O_7^{2-}$), 3.12 ns (**1** + 2,6-DC-4-NA) (Fig. 8). It is found that the fluorescence lifetime of the complexes has almost no change before and after quenching, which indicates that the fluorescence quenching phenomenon is mainly caused by the static quenching effect mechanism.[78]

4. Conclusions

To sum up, three new Cd-based complexes have been successfully synthesized. By tuning the length of spacers of three carboxylates, the structures of CPs **1–3** are changed from 2D 3,5-connected networks (CPs **1–2**) to 3D 3,5-connected framework (CP **3**). The deep analysis shows that the rational selection of spacers of dicarboxylates is proved to be an effective strategy to regulate structural details. The coordination polymers can be used as multifunctional sensors with good selectivity for metal cations (Fe^{3+}), anions (MnO_4^-, CrO_4^{2-}, $Cr_2O_7^{2-}$) and organochlorine pesticides (2,6-DC-4-NA), which proves that it is feasible path to construct stable and multi-response sensing materials after introducing pyridine amide ligands. Moreover, the study shows that the whole fluorescence quenching process is caused by the coexistence of fluorescence resonance energy transfer and static quenching effect mechanism. In the future, by optimizing the shape, size and testing environment of the materials will be the direction of our future efforts to improve the commercial application potential.

Conflicts of interest

The authors declare no competing financial interest.

Acknowledgements

This work was financially supported by the National Natural Science Foundation of China (21401010, 21971024), Education Department and the Natural Science Foundations of Liaoning province (LJ2020008, 2021-MS-312). Thanks to Professor Ninghai Hu (Changchun Institute of Applied Chemistry) for refining the crystal data structures.

References

1 D. F. He, S. M. Liu, F. J. Zhou, X. J. Zhao, Y. W. Liu, F. Luo and S. X. Liu, *RSC Adv.*, 2018, **8**, 34712–34717.
2 Q. Q. Xiao, G. Y. Dong, Y. H. Li and G. H. Cui, *Inorg. Chem.*, 2019, **58**, 15696–15699.
3 Q. Cheng and G. K. Zhang, *Tungsten*, 2020, **2**, 240–250.
4 A. Chowdhury, A. A. Khan, S. Kumari and S. Hussain, *ACS Sustainable Chem. Eng.*, 2019, **7**, 4165–4176.
5 K. Q. Zhao, L. K. Kong, W. W. Yang, Y. Huang, H. Li, S. H. Ma, W. J. Lv, J. Hu, H. L. Wang and H. L. Liu, *ACS Appl. Mater. Interfaces*, 2019, **11**, 44751–44757.
6 J. Z. Wang, H. Du, A. Olayiwola, B. Liu, F. Gao, M. L. Jia, M. H. Wang, M. L. Gao, X. D. Wang and S. N. Wang, *Tungsten*, 2021, **3**, 305–328.
7 Y. W. Li, J. Li, X. Y. Wan, D. F. Sheng, H. Yan, S. S. Zhang, H. Y. Ma, S. N. Wang, D. C. Li, Z. Y. Gao, J. M. Dou and D. Sun, *Inorg. Chem.*, 2021, **60**, 671–681.
8 L. Wang, H. X. Zhu, G. T. Xu, X. D. Hou, H. He and S. F. Wang, *J. Mater. Chem. C*, 2020, **8**, 11796–11804.
9 X. M. Tian, S. L. Yao, C. Q. Qiu, T. F. Zheng, Y. Q. Chen, H. P. Huang, J. L. Chen, S. J. Liu and H. R. Wen, *Inorg. Chem.*, 2020, **59**, 2803–2810.
10 D. K. Wang, M. Wang, K. X. Chen, Y. J. You, J. Zhang, X. H. Zhou and W. Huang, *Appl. Organomet. Chem.*, 2020, **34**, e5692.
11 X. Zhou, Y. X. Shi, C. Cao, C. Y. Ni, Z. G. Ren, D. J. Young and J. P. Lang, *Cryst. Growth Des.*, 2019, **19**, 3518–3528.

12 P. P. Guo, J. P. Sun, Z. Q. Xu, M. Liu, H. Li and Y. Wang, *J. Solid State Chem.*, 2019, **273**, 62–66.
13 X. Y. Zhao, B. Liang, K. C. Xiong, Y. W. Shi, S. L. Yang, T. Y. Wei, H. Zhang, Q. F. Zhang and Y. L. Gai, *Dalton Trans.*, 2020, **49**, 5695–5702.
14 T. Y. Gu, M. Dai, D. J. Young, Z. G. Ren and J. P. Lang, *Inorg. Chem.*, 2017, **56**, 4668–4678.
15 L. M. Fan, Y. J. Zhang, J. Wang, L. Zhao, X. Q. Wang, T. P. Hu and X. Y. Zhang, *Inorg. Chem. Commun.*, 2018, **89**, 32–36.
16 X. Lian and B. Yan, *Dalton Trans.*, 2016, **45**, 18668–18675.
17 Z. C. Sun, Y. Y. Liu and J. F. Ma, *Inorg. Chem. Commun.*, 2020, **122**, 108290–108296.
18 G. C. Liu, Y. Li, J. Chi, N. Xu, X. L. Wang, H. Y. Lin and Y. Q. Chen, *Dyes Pigm.*, 2020, **174**, 108064.
19 L. H. Wu, S. L. Yao, J. Li, H. Xu, T. F. Zheng, S. J. Liu, J. L. Chen and H. R. Wen, *CrystEngComm*, 2021, **23**, 482–491.
20 J. R. Zhang, J. J. Lee, C. H. Su, M. J. Tsai, C. Y. Li and J. Y. Wu, *Dalton Trans.*, 2020, **49**, 14201–14215.
21 X. L. Qu and B. Yan, *J. Mater. Chem. C*, 2020, **8**, 9427–9439.
22 B. Zhang, B. Li and Z. G. Wang, *ACS Sens.*, 2020, **5**, 162–170.
23 G. C. Liu, S. W. Han, Y. Gao, N. Xu, X. L. Wang and B. K. Chen, *CrystEngComm*, 2020, **22**, 7952–7961.
24 W. Talbert, D. Jones, J. Morimoto and M. Levine, *New J. Chem.*, 2016, **40**, 7273–7277.
25 J. Wang, N. N. Chen, C. D. Pan, C. Zhang and L. M. Fan, *New J. Chem.*, 2020, **44**, 9411–9418.
26 L. M. Fan, F. Wang, D. S. Zhao, X. H. Sun, H. T. Chen, H. W. Wang and X. T. Zhang, *Spectrochim. Acta, Part A*, 2020, **239**, 118467.
27 L. Q. Zhang, X. W. Wang, L. Gu, Y. H. Yu and J. S. Gao, *RSC Adv.*, 2020, **10**, 9476–9485.
28 S. H. Zhang, S. Y. Zhang, J. R. Li, Z. Q. Huang, J. Yang, K. F. Yue and Y. Y. Wang, *Dalton Trans.*, 2020, **49**, 11201–11208.
29 J. X. Ma, N. Xu, Y. Liu, Y. Wang, H. Li, G. C. Liu and X. L. Wang, *Inorg. Chem.*, 2020, **59**, 15495–15503.
30 Q. L. Guan, C. Han, F. Y. Bai, J. Liu, Y. H. Xing, Z. Shi and L. X. Sun, *Sens. Actuators, B*, 2020, **325**, 128767–128777.
31 C. J. Liu, T. T. Zhang, W. D. Li, Y. Y. Wang and S. S. Chen, *Crystals*, 2019, **9**, 664.
32 H. Q. Li, Z. Y. Ding, Y. Pan, C. H. Liu and Y. Y. Zhu, *Inorg. Chem. Front.*, 2016, **3**, 1363–1375.
33 M. Maruthupandi and G. Prabusankar, *RSC Adv.*, 2020, **10**, 28950–28957.
34 S. Kulovi, A. Pradhan, S. Maiti, H. Puschmann, E. Zangrando and S. Dalai, *ChemistrySelect*, 2020, **5**(11), 3337–3346.
35 S. R. Batten, B. L. Chen and J. J. Vittal, *ChemPlusChem*, 2016, **81**, 669–670.
36 L. J. Liu, Y. G. Ran, J. L. Du, Z. C. Wang, M. Liu and Y. J. Mu, *RSC Adv.*, 2021, **11**, 11266–11272.
37 Y. N. Wang, S. D. Wang, L. L. Yang, Y. F. Zhao and Q. F. Yang, *J. Solid State Chem.*, 2020, **289**, 121519–121525.
38 Y. Y. Liang, L. L. Xue, H. M. Hu, L. N. Zheng, X. F. Wang and G. L. Xue, *J. Solid State Chem.*, 2019, **276**, 6–18.
39 C. P. Li, W. W. Long, Z. Lei, L. Guo, M. J. Xie, J. Lü and X. D. Zhu, *Chem. Commun.*, 2020, **56**, 12403–12406.
40 S. Mukherjee, S. Ganguly, A. Chakraborty, A. Mandal and D. Das, *ACS Sustainable Chem. Eng.*, 2019, **7**, 819–830.
41 K. F. Chen, S. Yin and D. F. Xue, *Tungsten*, 2019, **1**, 287–296.
42 B. Ghanbari, L. Shahhoseini, A. Owczarzak, M. Kubicki, R. Kia and P. R. Raithby, *CrystEngComm*, 2018, **20**, 1783–1796.
43 J. W. Cui, S. X. Hou, K. V. Hecke and G. H. Cui, *Dalton Trans.*, 2017, **46**, 2892–2903.
44 L. L. Gao, Y. J. Bian, Y. Tian, Y. Q. Chen and T. P. Hu, *CrystEngComm*, 2020, **22**, 7046–7053.
45 H. Xu, B. Y. Zhou, K. Yu, Z. H. Su, B. B. Zhou and Z. M. Su, *CrystEngComm*, 2019, **21**, 1242–1249.
46 B. W. Schmidt, H. R. A. Jonker, T. Wulsdorf, H. D. Gerber, K. Saxena, D. Kudlinzki, S. Sreeramulu, G. Parigi, C. Luchinat, A. Heine, H. Schwalbe and G. Klebe, *J. Med. Chem.*, 2018, **61**, 5922–5933.
47 C. Dong, J. Q. Bai, X. L. Lv, W. Wu, J. Lv and J. R. Li, *Inorg. Chem.*, 2019, **58**, 15909–15916.
48 M. Kariem, M. Kumar, M. Yawer and H. N. Sheikh, *J. Mol. Struct.*, 2017, **1150**, 438–446.
49 J. Yang, J. F. Ma, Y. Y. Liu, J. C. Ma and S. R. Batten, *Inorg. Chem.*, 2007, **46**, 6542–6555.
50 X. L. Wang, Z. C. Guo, G. C. Liu, Y. Qu, S. Yang, H. Y. Lin and J. W. Zhang, *CrystEngComm*, 2013, **15**, 551–559.
51 G. C. Liu, J. Zhao, S. Liang, Y. Li, Z. H. Chang, X. L. Wang and B. K. Chen, *CrystEngComm*, 2021, **23**, 1263–1271.
52 Q. Q. Yan, B. Li, W. P. Jiang, Y. B. Xu, Z. Q. Xu and G. P. Yong, *J. Coord. Chem.*, 2020, **73**, 854–866.
53 Y. J. Wang, S. Y. Wang, Y. Zhang, B. Xia, Q. W. Li and Q. L. Wang, *CrystEngComm*, 2020, **22**, 5162–5169.
54 G. M. Sheldrick, *Acta Crystallogr., Sect. A: Found. Adv.*, 2015, **71**, 3–8.
55 T. Kumar, M. Venkateswarulu, B. Das, A. Halder and R. R. Koner, *Dalton Trans.*, 2019, **48**, 12382–12385.
56 T. Y. Xu, H. J. Nie, J. M. Li and Z. F. Shi, *Dalton Trans.*, 2020, **49**, 11129–11141.
57 J. M. Delente, D. Umadevi, S. Shanmugaraju, O. Kotova, G. W. Watson and T. Gunnlaugsson, *Chem. Commun.*, 2020, **56**, 2562–2565.
58 C. D. Si, D. C. Hu, Y. Fan, Y. Wu, X. Q. Yao, Y. X. Yang and J. C. Liu, *Cryst. Growth Des.*, 2015, **15**(5), 2419–2432.
59 Y. J. Mu, Y. G. Ran, B. B. Zhang, J. L. Du, C. Y. Jiang and J. Du, *Cryst. Growth Des.*, 2020, **20**(9), 6030–6043.
60 B. Dutta, A. Hazra, A. Dey, C. Sinha, P. P. Ray, P. Banerjee and M. H. Mir, *Cryst. Growth Des.*, 2020, **20**(2), 765–776.
61 S. S. Chen, Z. Y. Zhang, R. B. Liao, Y. Zhao, C. Wang, R. Qiao and Z. D. Liu, *Inorg. Chem.*, 2021, **60**(7), 4945–4956.
62 B. Li, Y. M. Zhao, A. Kirchon, J. D. Pang, X. Y. Yang, G. L. Zhuang and H. C. Zhou, *J. Am. Chem. Soc.*, 2019, **141**, 6822–6826.
63 X. L. Wang, Y. Xiong, X. T. Sha, G. C. Liu and H. Y. Lin, *Cryst. Growth Des.*, 2017, **17**, 483–496.
64 S. L. Hou, J. Dong, X. L. Jiang, Z. H. Jiao, C. M. Wang and B. Zhao, *Anal. Chem.*, 2018, **90**, 1516–1519.
65 X. S. Li, J. D. An, H. M. Zhang, J. J. Liu, Y. Li, G. X. Du, X. X. Wu, L. Fei, J. D. Lacoste, Z. Cai, Y. Y. Liu, J. Z. Huo and B. Ding, *Dyes Pigm.*, 2019, **170**, 107631–107671.

66 L. N. Ma, Y. K. Lu, W. J. Shi, L. Hou and Y. Y. Wang, *Inorg. Chem. Commun.*, 2019, **107**, 107490.
67 T. Gao, L. Zhao, L. L. Gao, J. Zhang, L. J. Zhai, X. Y. Niu and T. P. Hu, *Z. Anorg. Allg. Chem.*, 2019, **645**(14), 934–939.
68 W. J. Cai, Y. Liu, Y. Y. Ma, W. J. Wang, L. Hou and Y. Y. Wang, *Inorg. Chem. Commun.*, 2020, **113**, 107805.
69 B. Li, Q. Q. Yan and G. P. Yong, *J. Mater. Chem. C*, 2020, **8**, 11786–11795.
70 Q. Q. Xiao, Y. H. Li, D. Liu and G. H. Cui, *Inorg. Chem. Commun.*, 2020, **111**, 107665.
71 L. D. R. Vázquez, A. D. González and V. S. Mendieta, *Dalton Trans.*, 2021, **50**, 4470–4485.
72 Z. H. Wei, D. S. Chen, Z. F. Guo, P. Y. Jia and H. Z. Xing, *Inorg. Chem.*, 2020, **59**, 5386–5393.
73 J. Chi, B. Q. Zhong, Y. Li, P. P. Shao, G. C. Liu, Q. Gao and B. K. Chen, *Z. Anorg. Allg. Chem.*, 2021, **647**(12), 1284–1293.
74 V. Y. Borkhodoev, *J. Anal. Chem.*, 2016, **71**, 872–877.
75 S. Khelifi, F. Ayari, H. Tiss and D. B. H. Chehimi, *J. Australas. Ceram. Soc.*, 2017, **53**, 743–749.
76 C. Chen, X. L. Zhang, P. Gao and M. Hu, *J. Solid State Chem.*, 2018, **258**, 86–92.
77 L. J. Han, Y. J. Kong, G. Z. Hou, H. C. Chen, X. M. Zhang and H. G. Zheng, *Inorg. Chem.*, 2020, **59**, 7181–7187.
78 G. N. Liu, R. D. Xu, R. Y. Zhao, Y. Q. Sun, Q. B. Bo, Z. Y. Duan, Y. H. Li, Y. Y. Wang, Q. Wu and C. C. Li, *ACS Sustainable Chem. Eng.*, 2019, **7**, 18863–18873.